Journal of Rheology

Exploiting the lower disorder-to-order temperature in Polystyrene-*b*-Poly(*n*butyl acrylate)-*b*-Polystyrene triblock copolymers to increase their flow resistance at high temperature

Clément Coutouly[1], Evelyne van Ruymbeke[1*], Laurence Ramos[2], Philippe Dieudonné-George[2], Charles-André Fustin[1*]

1. Institute of Condensed Matter and Nanosciences (IMCN), Bio- and Soft Matter division (BSMA), Université catholique de Louvain, Place Pasteur 1 and Place Croix du Sud 1, Louvain-la-Neuve B-1348, Belgium

2. Laboratoire Charles Coulomb (L2C), Univ. Montpellier, CNRS, Montpellier, France,

**: charles-andre.fustin@uclouvain.be ; Evelyne.vanruymbeke@uclouvain.be*

ABSTRACT

This work focuses on the temperature dependent structural and rheological characterization of Polystyrene-*b*-Poly(*n*butyl acrylate)-*b*-Polystyrene triblock copolymers (PS-*b*-P*n*BA-*b*-PS) in the melt and in particular, on their ability to show a lower disorder-to-order temperature (LDOT). To this aim, copolymers of varying block length, but keeping the P*n*BA block as major component, were synthesized. Small-Angle X-ray Scattering revealed that the copolymers with short PS blocks (~10 kg/mol) approach a LDOT but do not cross it. At room temperature, these copolymers exhibit higher moduli compared to a P*n*BA homopolymer due to the reinforcing effect of the PS but are flowing at temperatures above the glass transition of the PS. Increasing the PS and P*nBA* block length, to keep the same PS fraction, induces more profound changes in the structural and viscoelastic behaviors. Such copolymer crosses the LDOT, leading to a microphase separated and ordered state at high temperature. Contrary to the copolymers with short PS blocks, the flow regime was not reached, even

at temperatures well above the glass transition of the PS. Instead, a low frequency plateau was observed in rheology, showing the increased lifetime of the microphase separated PS domains. ABA triblock copolymers exhibiting a LDOT behavior could thus be of interest for the design of thermoplastic elastomers or pressure sensitive adhesives that can resist flow at high temperatures.

I. INTRODUCTION

Block copolymers can form microphase-separated structures (lamellae, spheres,…) in bulk[1,2] or self-assemble into various structures (micelles, vesicles,…) in a selective solvent of one of the blocks.[3–6] ABA triblock copolymers, in particular, can form structures similar to their simpler AB diblock counterparts but are especially interesting because of the ability of the B block to form bridges between A domains. This capacity has a strong impact on the properties of the material.[7] Multi-block copolymers that use microphase separation to form a network are part of the so-called family of thermoplastic elastomers (TPEs). ABA thermoplastic elastomers exhibit interesting elastomeric properties like melting at high temperatures, extensibility, shape memory, and reprocessability.[8–10] Generally, ABA thermoplastic elastomers are constructed with a dominant B rubbery segment and smaller hard A blocks to form physical crosslinks with high strength and tunable modulus.[11,12] The hard domains provide good tensile and tear strength at room temperature, whereas the rubbery phase provides elastomeric properties such as flexibility and extensibility. Elastomers based on ABA copolymers have seen a growing interest in various applications, ranging from adhesives to clothing, automotive, and biomedical components.[13–15] For example, ABA copolymers with polystyrene as A block and polyisoprene or polybutadiene as B block offer improved optical transparency and stability to UV light.[16,17] In addition, acrylate-based triblocks exhibit excellent pressure-sensitive adhesive properties,[18,19] which can be tailored in function of the adhesive formulation.

It is well established that most TPEs owe their elastomeric properties to a microphase-separated structure, which affects both the mechanical and viscoelastic properties.[20–23] In particular, ABA triblocks can form different morphologies depending on their composition and degree of block incompatibility in bulk. The microphase-separated domains of hard A blocks often lead to the reinforcement of the sample, their elastic modulus being much higher than the rubbery plateau of the B blocks. Moreover, the B block can either form loops, so that the A blocks fold into the same microdomain, or form bridges between distinct A microdomains, which strongly affect the viscoelastic and tensile properties.[24]

While TPEs have excellent mechanical properties at room temperature, a major drawback of these systems is their rapid loss of tensile and tear strength at high temperatures,[25] limiting their range of applications. Amorphous TPEs are also flowing when heated above the Tg of the hard blocks. An

interesting way to address these limitations would be to design block copolymers that can microphase-separate upon a temperature increase, thus showing a lower disorder-to-order temperature (LDOT),[26] improving their temperature resistance. However, such transition is not common for block copolymers, contrary to an upper order-to-disorder transition (UODT), which easily takes place since at low temperature, the mixing entropy cannot overcome the unfavorable enthalpic interaction between the two blocks, thus leading to microphase separation. For example, a LDOT has been reported in three kinds of weakly interacting block copolymers: polystyrene-*b*-poly(*n*-alkyl methacrylate), poly(ethylene oxide)-*b*-poly(2-vinylpyridine), and poly(*n*-hexylnorbornene)-*b*-poly(cyclohexylnorbornene),[27–31] in which only van der Waals forces exist. The LDOT behavior of the two first systems has an entropic origin and has been attributed to differences in component compressibility. In such systems, the mixed state is indeed more densely packed than the microphase separated state.[32,33] With increasing temperature, a disorder-to-order transition is thus promoted due to the increase of the volume upon microphase separation, which induces an increase of the entropy. The behavior of the norbornene-based system was rather attributed to a different temperature-dependence of the solubility parameters for the two blocks. This property has been recently further exploited to design new LDOT block copolymers by introducing extra interactions such as H-bonding and Coulombic interactions to modulate the temperature dependence of the microphase separation, and to observe different behaviors such as a close-loop behavior or an order-to-order transition for example.[27,34–37]

In this work, we focus on ABA triblocks where the B soft central block is composed of low Tg (-53 °C) Poly(*n*-butyl acrylate) (PnBA), and the outer A blocks are made of moderately high Tg (100 °C) Polystyrene (PS).[38] We selected this pair of monomers because, as detailed below, PS/P*n*BA copolymers are known to exhibit a LDOT behavior in specific conditions. We investigate the relationships between the copolymer microstructure and their rheological properties as a function of temperature and copolymer composition. More precisely, the triblock copolymers have been designed to favor their microphase separation upon increasing temperature, thus offering the possibility to use these materials for applications such as temperature resistant pressure-sensitive adhesives or TPEs.

The microphase separation behavior of different types of PS-(meth)acrylate copolymers and their possible LDOT behavior has been previously studied in the literature. Russel et al.[33] were the first to report a LDOT behavior for styrene/*n*-butyl methacrylate (*n*BMA) diblock copolymers containing around 60 wt% of PS. They showed that the phase diagram was strongly dependent on the molar mass of the block copolymers. In particular, while a low molar mass copolymer (26 kg/mol) stays homogeneous whatever the temperature, a long copolymer (170 kg/mol) containing the same proportion of PS was found to be always microphase separated. In order to observe both a UODT and a LDOT within the same sample, a copolymer with an intermediate molar mass (99 kg/mol) had to be

used. The LDOT was observed at a high temperature (around 150 °C), and the UODT could take place since it is higher than the glass transition temperature (T_g) of the PS blocks.

Compared to PS-*b*-P*n*BMA block copolymers, copolymers based on PS and P*n*BA have a higher incompatibility between the blocks,[26] with a Flory-Huggins interaction parameter varying from 0.034 to 0.087 at room temperature.[39–44] For this reason, Mok et al.[32] reported that it is more difficult to observe a LDOT with these systems: while a block copolymer of molar mass 27 kg/mol is fully homogeneous, copolymers of 34 kg/mol are already too long and microphase separate in the whole range of temperatures studied.[45] The room to observe a LDO transition is thus very narrow. In order to circumvent this issue, the authors proposed to use gradient S/*n*BA copolymers as they have a lower driving force for microphase separation and hence have a better miscibility than the corresponding block copolymers. The gradient copolymers showed similar microphase transition behavior as the PS-*b*-P*n*BMA block copolymers, with a LDOT observed for copolymers of higher molar mass (of the order of 100 – 150 kg/mol). In addition, by tuning the magnitude of the S/*n*BA gradient, the authors showed that it is possible to adjust the transition temperature. Similar conclusion was found in ref. [46] where the authors compared the properties of random, gradient and block copolymers.

In the present work, we investigate the effects of the variation of block length, PS content, and temperature of PS-*b*-P*n*BA-*b*-PS triblock copolymers (named SAS in this paper) on their dynamics and viscoelastic properties in relation to their microphase separation behavior. Triblock copolymers have been chosen because they are a typical architecture used to prepare TPEs or PSAs. The triblock composition has been varied to promote a LDOT upon increasing temperature. As already mentioned, previous works on PS/P*n*BA systems showed that it is difficult to obtain LDOT behavior with block copolymers. [32,44] However, all these samples had a high PS content (around 60 wt%). Therefore, it seems important to verify if a decrease of the PS fraction to have a majority of P*n*BA, and thus ensure elastomeric properties, reduces the degree of microphase separation and favors a LDOT behavior.

To prepare PS-*b*-P*n*BA-*b*-PS triblock copolymers with low PS content, we developed a two-step synthetic procedure based on reversible addition-fragmentation chain transfer (RAFT) polymerization where we can easily vary the length of the PS outer blocks and of the P*n*BA central block to design well-defined triblock copolymers. This allows us to tune the microphase separation of the triblocks and study its impact on the dynamics of the systems at different temperatures. We investigate the relationship between the structural properties obtained by small-angle X-ray scattering (SAXS) and the linear viscoelastic properties obtained by rotational shear rheometry to understand how the sample properties can be modulated. Based on our first results, we then design a PS-*b*-P*n*BA-*b*-PS triblock copolymer that can still form physical bonds at high temperatures (165 °C) to create a stable network that can resist flow at elevated temperatures. This high-temperature resistance adds a new feature compared to typical TPEs or PSAs that melt or soften when the temperature is increased.

II. MATERIALS AND METHODS

II.1. Materials

The triblock copolymers were synthesized via RAFT polymerization in bulk. The full details are given in the supplementary information. The purified copolymers were analyzed using a combination of size exclusion chromatography (SEC) with polystyrene calibration, and ^{1}H NMR spectroscopy. The degree of polymerization of the P*n*BA block, and thus its molar mass, was determined by comparing the characteristic peaks of PS and P*n*BA in the ^{1}H NMR spectrum. The triblock characteristics are summarized in Table 1. The synthesis of the chain transfer agent, (1-Carboxy-1-methylethylsulfanylthiocarbonylsulfanyl)-2-methylpropionic acid, was achieved via a previously reported one-pot reaction as described in the SI.[33,34] A P*n*BA homopolymer, also synthesized by RAFT polymerization (see SI for details), was investigated as a reference sample.

Figure 1: Chemical structure of a PS-b-PnBA-b-PS triblock copolymer (named SAS in the paper) and its schematic representation.

II.2. Characterization methods

Small Angle X-ray Scattering (SAXS):

SAXS measurements were performed at different temperatures with an in-house setup of the Laboratoire Charles Coulomb, Université Montpellier, France. A high brightness low power X-ray tube, coupled with aspheric multilayer optics (GeniX3D from Xenocs), was employed. It delivers an ultralow divergent beam (0.5 mrad, λ=0.15418 nm). Scatterless slits were used to give a clean 0.6mm beam diameter with a flux of 35 Mphotons/s at the sample. We worked in a transmission configuration, and scattered intensity was measured by a 2D "Pilatus" 300K pixel detector by Dectris (490*600 pixels) with a pixel size of 172×172 μm^2, at a distance of 1.9 m from the sample. All Intensities were corrected by transmission, and the empty cell contribution (two mylar foils) was subtracted. For each temperature, ten scans of 30 min were performed, and a Mettler F12 stage was employed to control the sample temperature.

Linear viscoelasticity:

Rotational shear rheological experiments were performed in the linear regime on an ARES (TA Instruments) strain-controlled rheometer equipped with an oven. All experiments were carried out at given temperatures, using 8 mm plate-plate geometries. The gap was adjusted between 0.8 and 1 mm to fill the geometry. All samples were equilibrated for about an hour in the rheometer at a temperature of 130 °C, and normal forces were checked to be relaxed prior to any measurement. Samples were measured at several temperatures from T= -20 to 200 °C, depending on the samples. Measurements were conducted from both high to low and low to high temperatures to check the reversibility of the measurements. For the triblock master curves, the association of the PS blocks depends on temperature, and it is thus expected that the triblocks exhibit thermorheological complexity.

Dynamic mechanical analysis:

Dynamic mechanical analyses were performed with a DMTA/SDTA861e from Mettler Toledo (Greifensee, Switzerland). Disc specimens of 6 mm diameter and 0.5 mm thickness were heated from -70 to 200 °C at 3 °C/min for the samples $S_{12}A_{35}S_{12}$, $S_{12}A_{62}S_{12}$, $S_{10}A_{100}S_{10}$, and P*n*BA, while the heating rate was 1 °C/min for the sample $S_{25}A_{120}S_{25}$. The samples were analyzed under shear at a constant frequency of 1 Hz, a constant force of 0.1 N, and by a maximum strain imposed of 0.2%.

Table 1: Composition parameters of PS-b-PnBA-b-PS triblock copolymers and of the PnBA reference.

Sample[a]	Name	Components		PS content (wt%)	Đ
		Mn_{PnBA} (kg/mol)[b]	Mn_{PS} (kg/mol)[c]		
PS12k-*b*-PnBA35k-*b*-PS12k	$S_{12}A_{35}S_{12}$	35	25	42	1.45
PS12k-*b*-PnBA62k-*b*-PS12k	$S_{12}A_{62}S_{12}$	62	25	29	1.45
PS10k-*b*-PnBA97k-*b*-PS10k	$S_{10}A_{100}S_{10}$	97	19	16	1.5
PS25k-*b*-PnBA120k-*b*-PS25k	$S_{25}A_{120}S_{25}$	120	49	29	1.5
PnBA	PnBA	95	/	0	1.18

[a] The numbers indicate the number averaged molar mass of the corresponding block in g/mol.

[b] Molar mass of the P*n*BA block determined by ^{1}H NMR.

[c] Molar mass of the PS macro-CTA determined by SEC (PS standards calibration).

III. RESULTS AND DISCUSSION

III.1. Properties of SAS block copolymers composed of short PS blocks

A. Structuration of the SAS triblock copolymers

As mentioned in the Introduction, the objective is to synthesize triblock copolymers with a major P*n*BA block to favor a LDOT behavior. To this end, short PS blocks of molar mass around 10-12 kg/mol have been selected. Since the microphase separation depends on the sample composition, P*n*BA central blocks of different molar mass (35 kg/mol, 62 kg/mol, and 97 kg/mol) have been synthesized (see Table 1).

The influence of the presence of the PS blocks on the sample microphase separation can be first detected by looking at the glass transition temperatures (T_g) obtained by DMA. For P*n*BA and PS homopolymers, the glass transition temperatures reported in the literature are T_g =-53 °C for a P*n*BA with a molar mass of around 100 kg/mol,[47] and for PS, T_g varies between 90 °C to 105 °C for molar masses between 12 and 25 kg/mol.[48] The data obtained by DMA for our triblock copolymers are presented in Figure 2.

Figure 2: a) DMA data of SAS copolymers, b) corresponding Tan δ. Temperature sweep tests have been performed under oscillatory shear at a frequency of 1 Hz.

At low temperature, all samples have very high, and more or less constant, moduli (despite some scattering in the experimental data), indicating that they are all in the glassy state. The moduli then decrease with temperature. For the three triblocks, the first drop in moduli occurs at a higher temperature compared to the P*n*BA homopolymer and depends on the PS fraction: the higher the PS fraction, the higher the temperature where this first modulus drop occurs. This is also seen in Figure 2b by the shift of the tanδ peak toward high temperature with increasing PS fraction. Moreover, the broadness of the tanδ peak changes with the sample composition. While it is rather sharp for the P*n*BA homopolymer, it is broader for the copolymers. At temperatures around 100-120 °C a second modulus drop occurs, leading to the flow of the samples as indicated by the crossover between the storage, G', and the loss, G", moduli. For the $S_{12}A_{35}S_{12}$ sample, the two modulus drops are barely noticeable and almost merge into a single drop. These observations suggest that the triblocks are weakly segregated or in the composition fluctuation regime. Indeed, if the samples were microphase separated, two clear tanδ peaks would be observed at the glass transition temperatures of the pure P*n*BA and pure PS.[44,46] On the other hand, if the samples were fully homogenous, a single clearly marked tanδ peak would

occur at an intermediate temperature. Here, an intermediate situation is observed. For the $S_{12}A_{62}S_{62}$ and the $S_{10}A_{100}S_{10}$ samples, a first T_g is observed at low temperature but above the T_g of pure P*n*BA (-53 °C) and with a much broader tanδ peak as explained above. The second drop in modulus at high temperature probably starts at the T_g of the PS even if no associated tanδ peak is seen in Figure 2b. These two triblocks show thus some degree of segregation. On the other hand, the two drops of modulus for the $S_{12}A_{35}S_{12}$ sample almost merge into a single one, indicating a more homogeneous sample characterized by a smaller amplitude of the composition fluctuations. Finally, it is interesting to note that at room temperature, which would be the usage temperature of these materials, the elastic moduli of the three copolymers are very different, covering about two orders of magnitude. Tuning the degree of segregation of the sample has thus an important impact on the mechanical properties and thus on the selection of potential applications.

Since DMA revealed differences in the sample microphase-separation, the structuration of the triblock copolymers was then analyzed by SAXS. We first investigate the microstructure of $S_{10}A_{100}S_{10}$ sample, which contains the lowest fraction of PS. DMA measurements suggested that this sample exhibits composition fluctuations. It must be noted here that a weak scattering intensity is expected for these triblocks due to the small electron density difference between PS (0.565 mol/cm^3) and P*n*BA (0.590 mol/cm^3). The scattering profiles of the $S_{10}A_{100}S_{10}$ sample are shown in Figure 3 for different temperatures in the range 25-92°C. A single, weak and broad peak is observed around 0.25 nm^{-1} at room temperature, compatible with composition fluctuations and in good agreement with the DMA results.[49–53]

As expected, the intensity of the SAXS peak increases gradually with temperature while the peak position stays fixed (Figure 3). This is not an annealing effect since the peak intensity goes back to its initial level upon cooling the sample (See SI, Figure S1). This increase of the SAXS peak intensity with an increase in temperature indicates that the amplitude of the composition fluctuations in the $S_{10}A_{100}S_{10}$ sample increases with temperature, suggesting that the sample approaches the order-to-disorder temperature (LDOT).[54] This finding is in contrast with the results of Mok et al., who reported that a LDOT could not exist for diblock copolymers of large molar mass (> 34 kg/mol).[32] However, the copolymers studied had a much higher PS fraction, around 60-70%. Our results unambiguously show that it is possible to approach a LDOT, provided that the PS blocks are short, and the PS fraction is rather low, i.e., P*n*BA should be the major component. Our results are consistent with the ones obtained by Pakula et al., who reported an increase of the SAXS peak intensity in SAS asymmetric triblocks upon an increase in temperature, but mistook this increase for an annealing effect since they did not record the SAXS data upon cooling back the sample to room temperature.[55] Thus, the amplitude of the composition fluctuations increases with temperature, but no high-order peaks are

present in the scattering profiles, showing the absence of long-range correlation. Therefore, while the system evolves toward a more structured state, the ODT is not crossed, and the sample remains disordered.

Figure 3: SAXS data of the $S_{10}A_{100}S_{10}$ sample from 25 °C to 92 °C. The insert corresponds to the peak maximum intensity as a function of temperature.

In order to further investigate the temperature dependence of the microstructure of SAS triblock copolymers, SAXS profiles at different temperatures for the $S_{12}A_{35}S_{12}$ and $S_{12}A_{62}S_{12}$ samples have been collected (Figure 4). The PS block length of these two samples is comparable to that of the $S_{10}A_{100}S_{10}$ sample, but they have a larger PS fraction since the P*n*BA block is shorter. At 20°C, the $S_{12}A_{35}S_{12}$ sample shows no peak in SAXS, but a weak and broad peak appears around 40°C which intensity then increases up to 80 °C (see Figure 4a). Then, its intensity continues to slowly increase with temperature, indicating that this sample also tends towards a LDOT, albeit more weakly than the other copolymers. At room temperature, there is thus no or very weak composition fluctuations and their amplitude weakly increases with temperature. This behavior is globally similar to the $S_{10}A_{100}S_{10}$ sample, but since the $S_{12}A_{35}S_{12}$ sample has the smallest molar mass, it has the lowest incompatibility between the blocks (as also observed in DMA, see Figure 2), and the composition fluctuation amplitude starts to increase at higher temperatures. Finally, for the third sample, $S_{12}A_{62}S_{12}$ (Figure 4b), an intermediate behavior compared to the ones of the $S_{10}A_{100}S_{10}$ and $S_{12}A_{35}S_{12}$ samples is observed, in good agreement with the DMA results.

Figure 4: SAXS data on a) $S_{12}A_{35}S_{12}$, and on b) $S_{12}A_{62}S_{12}$ at temperatures from 20 °C to 120 °C. The insert corresponds to the peak maximum intensity as a function of temperature.

The SAXS data of the three block copolymers are then compared in Figure S2 at specific temperatures. As already mentioned, the SAXS peak intensity increases with temperature for all the triblock copolymers. In Figure S2b, it is also seen that the distance associated with the SAXS peak correlates with the length of the P*n*BA block: the longer the P*n*BA block, the smaller the q value of the SAXS peak (larger associated distance). To have a better insight about these values, we estimated the end-to-end distances of a SAS triblock chain in a fully stretched conformation and for the freely rotating chain model where the long-distance self-interactions are not considered. We compared them to the average distance corresponding to the SAXS peak ($d_{SAXS}=2\pi/q_{peak}$, where q_{peak} is the peak position). The end-to-end distance of a fully stretched linear SAS copolymer chain can be estimated by:

$$L_{zig-zag}(nm) = Nb \sin\left(\frac{\tau}{2}\right), \quad (1)$$

Where N is the number of C-C bonds in the copolymer chain, b is the length of a C-C bond (0.159 nm) and τ is the angle of a C-C-C bond (109.5°). On the other hand, the freely rotating chain model for a linear SAS copolymer chain is calculated from:

$$L_{frc}{}^2(nm) = C_\infty N b^2 \quad (2)$$

Where C_∞ is the characteristic ratio of the copolymer chain. Since the C_∞ of PS and P*n*BA are rather close ($C_{\infty,PnBA}$ = 10,1 and $C_{\infty,PS}$ = 10,8),[56] an average value for C_∞, calculated based on the triblock composition, was used. The results are shown in Table 2.

Table 2: d_{SAXS} is the distance measured by SAXS, L_{frc} is the calculation of the end-to-end distance with the freely rotating chain model, and $L_{zig-zag}$ is the model used for the end-to-end distance calculation for a fully stretched polymer chain.

Sample	$S_{12}A_{35}S_{12}$	$S_{12}A_{62}S_{12}$	$S_{10}A_{100}S_{10}$
d_{saxs} (nm)	18	25	29
L_{frc} (nm)	14	18	22
$L_{zig-zag}$ (nm)	137	185	252

For all triblocks, the calculated end-to-end distances of freely rotating chains agree relatively well with the distances measured in SAXS, even if they are a bit lower. This shows that the triblocks are in a random coil conformation, possibly slightly stretched, in good agreement with the composition fluctuation regime.[44] Since the PS block length in these samples is almost constant, the characteristic distances mainly scale with the P*n*BA block length.

B. Viscoelastic properties of SAS triblock copolymers

Changes in the sample microphase separation of copolymers can strongly affect their linear viscoelastic properties, as reported by Bates for example.[57] Therefore, we investigated the temperature-dependent linear viscoelastic (LVE) behavior of the three triblocks. Results are summarized in Figure 5, which shows the storage and loss moduli of the copolymers at given temperatures compared to the data of a P*n*BA homopolymer sample

At low temperature, T = 0 °C, the frequency sweep data reveal that the level of the plateau modulus of the triblock copolymers strongly increases with the PS fraction, taking values that can be several orders of magnitude larger than the rubbery plateau of the P*n*BA homopolymer estimated at

160 kPa.[58,59] The increase in modulus depends on the PS fraction, the higher the PS content the larger the modulus, in agreement with the DMA data (see Figure 2). This reinforcement effect is attributed to the high modulus of the glassy state of the PS. The slight decrease of the storage modulus at low frequency is attributed to the local equilibration of the P*n*BA matrix. At 25 °C, the general behavior is similar to the one at 0 °C, with the level of the elastic plateau following the PS fraction in the samples. Moreover, while the P*n*BA homopolymer reaches its terminal regime of relaxation, the triblock copolymers do not flow (G' is till larger than G"). The $S_{12}A_{35}S_{12}$ sample shows a much higher elastic plateau than the two other copolymers because this sample has not yet reached its softening temperature, as observed in the DMA data (Figure 2)

Figure 5: Linear rheology at 0 °C, 25 °C, 60 °C and 100 °C of PnBA95k homopolymer (green curves), $S_{10}A_{100}S_{10}$ (blue curves), $S_{12}A_{62}S_{12}$ (red curves) and $S_{12}A_{35}S_{12}$ (pink curve). Above 40 °C, PnBA is in the flowing regime.

At 60 °C, the viscoelastic behavior of the $S_{10}A_{100}S_{10}$ and $S_{12}A_{62}S_{12}$ triblocks qualitatively changes, with the appearance of a $\omega^{1/2}$ dependence of the storage and loss moduli in the low-frequency region. This transition results from two opposing effects. On the one hand, the PS starts to soften. As it does not reinforce the sample anymore, the plateau modulus of the triblock copolymers drops, and reaches values close to the room temperature rubbery plateau of an entangled P*n*BA homopolymer (160 kPa [58,59]). This softening of the PS also allows the relaxation of the P*n*BA entanglements. On the other hand, as shown by the SAXS data, the amplitude of the composition fluctuations increases with temperature. This tends to limit the relaxation of the P*n*BA chains, which are trapped between PS-rich regions. The net result is that, at this temperature, the viscoelastic response of the sample is mostly dominated by the entanglements of the P*n*BA chains, which are unable to fully relax since their chain extremities are trapped into PS-rich regions that act as physical crosslinking points. The linear rheological response of the $S_{12}A_{35}S_{12}$ sample at 60 °C is slightly different, showing higher modulus values and a continuous decrease in the storage and loss moduli with a $\omega^{1/2}$ dependence over the whole frequency range. This behavior is attributed to the higher softening temperature of the P*n*BA of the $S_{12}A_{35}S_{12}$ sample (see Figure 2), which occurs in the high frequency region at 60 °C, and is directly followed by the softening of the PS.

Finally, at 100 °C, all samples show a transition from a solid-like to a liquid-like behavior. Their flow regime reflects the ability of the chains to disentangle, which mainly depends on two factors. First, it depends on the probability of a PS block to escape from the PS-rich regions. While increasing the temperature leads to an increase of the amplitude of the composition fluctuations (see Figures 3 and

4), we observe, however, that the relaxation of the samples is accelerated. This suggests that, at this temperature, the lifetime of the PS-rich regions is decreasing. Second, it depends on the length of the P*n*BA chains. The more they are entangled, the longer will be their relaxation time. Considering that the molar mass between two entanglements is 18 kg/mol,[58,59] the $S_{10}A_{100}S_{10}$, $S_{12}A_{62}S_{12}$, and $S_{12}A_{35}S_{12}$ samples contain around 6.5, 4.8, and 3.2 entanglements per P*n*BA chain, respectively.

In order to further highlight the structural modification taking place in the block copolymers with increasing temperature, we plot in Figure 6 the evolution of the storage modulus G' as a function of the loss modulus G", following the method proposed by Han et al.[60,61] Such plot can be seen as an alternative method to the Time-Temperature Superposition principle, for which a good overlap of data taken at different temperatures means that the temperature only affects the segmental dynamics of the material. Overall, the curves of the triblocks superimpose quite well at low temperature, which indicates that there is no structural or phase change in the material, only the expected evolution of the dynamics with temperature. However, a deviation is observed at higher temperatures. For the $S_{12}A_{62}S_{12}$ and $S_{10}A_{100}S_{10}$ samples, the level of G' lowers with increasing temperature. As G' is well below the entanglement plateau modulus of the P*n*BA, this result suggests that, in this temperature range, increasing the temperature leads to a slightly lower fraction of P*n*BA segments trapped by the PS, which can be attributed to the increased dynamics of the PS segments, which dominates over the effect of stronger composition fluctuations. On the other hand, for the $S_{12}A_{35}S_{12}$ sample, the opposite trend is observed for intermediate loss moduli. This can be understood based on the higher softening temperature of its P*n*BA (see Figure 2): at high temperature (T > 80-100 °C) the segmental dynamics of the P*n*BA is still too slow to overcome the sample structuration induced by increased composition fluctuations.

Figure 6: Han's plot for the reference triblock a) $S_{12}A_{35}S_{12}$, b) $S_{12}A_{62}S_{12}$, and c) $S_{10}A_{100}S_{10}$.

These LVE results show that despite the temperature-induced increase of the amplitude of the composition fluctuations, these triblock copolymers are flowing at high temperatures and do not reach an elastomeric-like behavior. This indicates that, although the samples approach their LDOT when increasing temperature, this transition is never reached. Therefore, as described in the following Section, a triblock copolymer containing longer PS blocks was synthesized and characterized. In order to favor its LDO transition, a very long P*n*BA block was used to keep the volume fraction of PS below 50%.

III.2. Properties of a SAS block copolymer composed of longer PS blocks

A. Structural properties

Based on the SAXS and rheology results described for triblock copolymers with short PS blocks, we synthesized a new copolymer, $S_{25}A_{120}S_{25}$, with longer outer and central blocks in order to induce a microphase separation with increasing temperature. The long, entangled, P*n*BA middle block should exhibit good elastomeric properties, while the longer PS blocks should provide a longer lifetime of the PS domains, even at high temperatures, that should prevent the material from flowing. Figure 7 presents the DMA data of this sample in comparison to the $S_{12}A_{62}S_{12}$ sample, which contains the same PS fraction, and to the P*n*BA homopolymer.

Figure 7: a) DMA data of the $S_{12}A_{62}S_{12}$ and $S_{25}A_{120}S_{25}$ copolymers and of the PnBA homopolymer, b) corresponding Tan δ*. Temperature sweep tests have been performed under oscillatory shear at a frequency of 1 s^{-1} and an amplitude of 1%.*

The $S_{25}A_{120}S_{25}$ sample shows two well-separated peaks in the tanδ curve, corresponding to the T_g values of the P*n*BA and PS blocks, at values close to the corresponding homopolymers (note that the PS T_g is a bit overestimated, 120°C from the tanδ peak, as often in DMA measurements compared to DSC). [55] On the opposite, the $S_{12}A_{62}S_{12}$ sample shows only a broad tanδ peak as previously discussed. This indicates that the $S_{25}A_{120}S_{25}$ sample is better microphase-separated than the other triblock copolymer. Moreover, contrary to our findings for the triblock copolymers with shorter PS chains, the flow regime of the $S_{25}A_{120}S_{25}$ sample (with G" > G') is not observed, even at very high temperatures well above the T_g of the pure PS blocks. This indicates that at these high temperatures, a part of the P*n*BA blocks is still unable to disentangle and relax, most probably due to the existence of stronger microphase separated domains between which the P*n*BA blocks are trapped. From these results, we can estimate the maximum usage temperature of this copolymer by applying the Dahlquist criterium (G' should be below 0.1 MPa). This criterium, often used in adhesive formulations, defines the maximum temperature that can be reached before obtaining a sticky material. [62] From Figure 7, the maximum usage temperature of the $S_{25}A_{120}S_{25}$ sample would be 165 °C. At this stage, it is unclear whether these presumed microphase separated domains are already present at low temperatures or if they only appear at high temperatures due to the crossing of the LDOT. In order to address this question, SAXS measurements have been performed.

Figure 8 shows the SAXS profiles obtained for this sample at temperatures from 25 °C to 200 °C. At 25 °C, no peak is observed in the SAXS analysis. This observation is difficult to rationalize since a better degree of microphase separation was expected for this sample considering its composition and based on the DMA results. This could suggest that despite the larger immiscibility of the blocks, the contrast between the P*n*BA and the PS regions is still too weak to be detected by SAXS. However, as

soon as the temperature is increased to 50 °C, a peak appears in the SAXS data, with higher relative intensity compared to the other triblocks (Figure S3). This larger intensity indicates a larger amplitude of composition fluctuations for this sample. The peak intensity further increases with increasing temperature up to 100 °C and reaches very large values. Above 100 °C, another regime is observed, in which the peak gradually shifts to lower q values with temperature up to 200 °C, indicating an increase of the characteristic distance. This shift in peak position was not observed for the other three triblocks. As previously done, we calculated the end-to-end distance by the freely rotating chain model (see Equation 2) for this triblock and found 29 nm. The distance corresponding to the SAXS peak position is d_{SAXS}= 42 nm in the regime up to 100 °C, where the peak position does not vary with temperature and reaches a value of d_{SAXS}= 71 nm at 200 °C. The greater discrepancy between the calculated and experimental values compared to the other triblocks indicates a larger degree of chain stretching than for the other triblocks, in agreement with a better microphase separation.[44]

The much larger characteristic distance observed above 100 °C (up to 71 nm at 200 °C) indicates that more profound structural changes occur for this sample as compared to the other triblocks. While the shift in the peak position could be partially due to the thermal expansion of the sample taking place with increasing temperature, it could also be due to a gradual change of the structure as the sample is becoming more ordered. Indeed, while up to 100 °C, the sample stays in a disordered state (composition fluctuation regime), at higher temperatures, it starts to become more ordered, as confirmed by the apparition of a high-order peak at high q from 125 °C, which shifts to lower q when temperature increases, following the shift of the main peak. While its intensity is rather low, this peak is observed around $\sqrt{3}$ q*, with q* being the position of the main peak, possibly indicating a hexagonally packed cylinders morphology, compatible with the PS fraction of 29% (Figure S4). Contrary to the other triblocks, it is thus possible that the T_{DOT} is crossed in this case. As for the other three copolymers, the evolution of the SAXS peak intensity with temperature is fully reversible (see Figure S5).

Figure 8: SAXS data of $S_{25}A_{120}S_{25}$ sample at temperatures from 25 °C to 200 °C. The insert corresponds to the evolution of the peak position q (▲) versus the temperature.*

B. Viscoelastic properties

The $S_{25}A_{120}S_{25}$ sample shows a different structural behavior at elevated temperatures compared to the previous triblocks studied. It is thus interesting to see if this difference also translates into its viscoelastic behavior. It will be particularly interesting to compare the $S_{25}A_{120}S_{25}$ and $S_{12}A_{62}S_{12}$ samples

since both have the same PS fraction, but the length of all the blocks of the $S_{25}A_{120}S_{25}$ triblock is two times larger.

Figure 9 presents the frequency sweeps recorded at different temperatures for the $S_{25}A_{120}S_{25}$ and $S_{12}A_{62}S_{12}$ triblocks and for the P*n*BA homopolymer. At 0 °C and 25 °C, the $S_{25}A_{120}S_{25}$ sample exhibits a plateau modulus, which is higher than the one of the P*n*BA homopolymer due to the rigid PS reinforcing the P*n*BA. However, this reinforcement effect is weaker than in sample $S_{12}A_{62}S_{12}$. This is consistent with the DMA data, which showed that the glass transition of the P*n*BA is taking place at a lower temperature for $S_{25}A_{120}S_{25}$ than for $S_{12}A_{62}S_{12}$ due to its microphase separation, and, consequently, to its purer P*n*BA phase.

An important difference between the two triblocks can also be observed at 60 °C and 100 °C. While the $S_{12}A_{62}S_{12}$ sample goes through a transition leading to its flow regime at 100 °C, for the $S_{25}A_{120}S_{25}$ sample, a transition leading to a second, low-frequency, plateau occurs at 60 °C. This low-frequency plateau persists at 100 °C despite the fact that the glass transition of the pure PS is reached. This indicates that PS-rich regions are formed at high temperature, which are stable enough to prevent the relaxation of the copolymer chains, i.e., the microphase separated domains which appear at high temperature exhibit a long lifetime. This is in good agreement with the SAXS data (Figure 8) which showed a change of regime from around 100°C, where the sample reaches a microphase separated state.

Figure 9: Linear rheology at 0 °C, 25 °C, 60 °C, and 100 °C of the PnBA homopolymer (green curves), and of the $S_{12}A_{62}S_{12}$ (red curves), and $S_{25}A_{120}S_{25}$ (black curves) copolymers.

In order to better highlight the sample evolution at high temperatures, the thermorheological complexity of the $S_{25}A_{120}S_{25}$ triblock is studied in Figure 10. To this end, dynamic rheological measurements were carried out in a temperature range from -20 °C to 200 °C. The time-temperature superposition (TTS) principle was first used on the P*n*BA homopolymer to create a master curve at a reference temperature T_{ref}= 25 °C. Horizontal shift factors were fitted with the WLF equation[63] (Equation 3) at T_{ref}= 25 °C, using the constants c_1= 6.2 and c_2=131.17 K proposed in Ref. 57.

$$\log a_T = \frac{-c_1(T - T_r)}{c_2 + (T - T_r)} \tag{3}$$

Where a_T is the WLF shift factors, T is the temperature, T_r is the reference temperature used to construct the master curve, and c_1, c_2 are empirical constants adjusted to fit the values of the superposition parameter a_T.

We then used the same c_1 and c_2 coefficients to determine the shift factors for the $S_{25}A_{120}S_{25}$ triblock. This requires considering a new reference temperature for sample $S_{25}A_{120}S_{25}$ to ensure that the master curves of both samples are built at iso-T_g condition (i.e., $T_{ref} - T_g$ = constant). [64] A very good superposition of the low temperature curves is found by considering $T_{ref}(S_{25}A_{120}S_{25})$= 32 °C, which corresponds to an increase of 7 °C of the P*n*BA Tg value, compared to the reference sample. The master curve for the $S_{25}A_{120}S_{25}$ triblock built with these shift factors is very good at high and intermediate frequencies, however, it fails at low frequencies, where the level of the second plateau varies with the temperature.

The second, low-frequency plateau is visible from temperatures above ca. 40 °C, and its level does not vary up to 80 °C. Above this temperature, its level progressively decreases until 130 °C. The 80-130 °C temperature range corresponds to the softening of the PS, which becomes able to reorganize, leading to microphase separation, as supported by the SAXS data (Figure 8). Thus, we can conclude that in the 80-130 °C range, the storage modulus decreases because the appearance of the microphase separation does not allow to fully compensate for the increased dynamics of the PS segments. Nevertheless, this compensation is much better for the $S_{25}A_{120}S_{25}$ triblock than for the other samples since it is not flowing at these high temperatures, contrary to the latter. This is attributed to its longer PS blocks and the larger stability of the microphase separated PS domains, the other triblocks being only in the composition fluctuation regime at high temperature.

Between 130 °C and 200 °C, the level of the second plateau stays constant. This is an unusual behavior for block copolymers, as it suggests that the stability of the PS domains is not reduced with increasing temperature. In this temperature regime, the SAXS data shows that the sample keeps on ordering as indicated by the appearance of a high-order peak (Figure 8). Therefore, we can conclude that the LDOT prevents the sample from flowing at high temperatures, giving rise to a high-temperature resistant block copolymer.

Figure 10: $S_{25}A_{120}S_{25}$ master curve (T_{ref}= 32 °C) vs PnBA homopolymer (T_{ref}= 25 °C) based on the c_1 and c_2 determined for the pristine PnBA master curve and created at iso-Tg.

Figure 11 presents the Han plot for the $S_{25}A_{120}S_{25}$ sample. Similar conclusions as from the master curve can be drawn, with the first regime from -20 °C to around 80 °C where the curves superimpose, then a second regime from 80 °C to 130 °C, where the offset between the curves gets larger and larger as the temperature increases, and, finally, a third regime above 130 °C where the low-frequency plateau is strengthened.

Figure 11: Han's plot for the sample $S_{25}A_{120}S_{25}$.

IV. CONCLUSION

In this work, we have exploited the possibility of achieving a lower disorder-to-order temperature (LDOT) behavior with PS-*b*-P*n*BA-*b*-PS triblock copolymers to evaluate the potential utility of such materials as temperature resistant thermoplastic elastomers. To this aim, we have first synthesized three triblock copolymers with short PS blocks (around 10-12 kg/mol) and a P*n*BA major block of different length. SAXS and rheology showed that an increase of temperature leads to an increase of the amplitude of the composition fluctuations, but these samples only tend to the LDOT and stay in the disordered state. The copolymers showed a high modulus at room temperature due to the reinforcing effect of the PS but flowed at temperatures above the glass transition of the PS because the faster segmental dynamics of the PS blocks dominates over the better structured morphology of the sample. Another triblock copolymer was thus designed to ensure the crossing of the LDOT, leading to a microphase separated state, and thus to a longer lifetime for the PS domains. Longer PS outer blocks were thus used, but the P*n*BA block length was also increased to keep a relatively low PS fraction to be able to reach the LDOT. As expected, this copolymer crossed the LDOT and was microphase separated at high temperature, while keeping the reinforcement effect at room temperature. However, contrary to the first three copolymers, the flow regime of this longer copolymer was not reached, even at very high temperatures well above the glass transition of the PS. Instead, a plateau was observed in rheology, showing the increased lifetime of the microphase separated PS domains. These observations show that PS-*b*-P*n*BA-*b*-PS triblock copolymers are potentially interesting candidates for developing TPEs that can keep their elastomeric properties even at high temperatures, around 165 °C in the present case, provided that the copolymer composition is appropriately adjusted. Tensile tests at high temperature will have of course to be performed to confirm the potential use of these triblock copolymers as TPEs. These copolymers could find applications in diverse areas since they combine good mechanical properties at room temperature and improved resistance to flow at elevated temperatures.

SUPPLEMENTARY MATERIAL

Full details on copolymer synthesis, additional SAXS and DMA graphs, master curves for some copolymers.

ACKNOWLEDGMENTS

This work was funded by the EU (Horizon 2020, Marie Skłodowska-Curie ITN DoDyNet, Grant Agreement No. 765811). E.V.R. is Research Associate of the FRS-FNRS.

References

[1] Li, M.-H.; Keller, P.; Yang, J.; Albouy, P.-A., "An Artificial Muscle with Lamellar Structure Based on a Nematic Triblock Copolymer," Adv. Mater. 16, 1922–1925 (2004).

[2] Howse, J. R.; Topham, P.; Crook, C. J.; Gleeson, A. J.; Bras, W.; Jones, R. A. L.; Ryan, A. J. "Reciprocating Power Generation in a Chemically Driven Synthetic Muscle," Nano Lett. 6, 73–77 (2006).

[3] Karatzas, A.; Talelli, M.; Vasilakopoulos, T.; Pitsikalis, M.; Hadjichristidis, N., "Micellization of ω-Functionalized Diblock Copolymers in Selective Solvent. Study on the Effect of Hydrogen Bonds," Macromolecules 39, 8456–8466 (2006).

[4] Lau, B. K.; Wang, Q.; Sun, W.; Li, L., "Micellization to Gelation of a Triblock Copolymer in Water: Thermoreversibility and Scaling," J. Polym. Sci. Part B Polym. Phys. 42, 2014–2025 (2004).

[5] Mai, Y.; Eisenberg, A., "Self-Assembly of Block Copolymers," Chem. Soc. Rev. 41, 5969 (2012).

[6] Karayianni, M.; Pispas, S., "Self-Assembly of Amphiphilic Block Copolymers in Selective Solvents. In Fluorescence Studies of Polymer Containing Systems," Springer International. 16, 27–63 (2016).

[7] Arun, A.; Dullaert, K.; Gaymans, R. J., "The Melt Rheological Behavior of AB, ABA, BAB, and $(AB)_n$ Block Copolymers with Monodisperse Aramide Segments," Polym. Eng. Sci. 50, 756–761 (2010).

[8] Hentschel, J.; Kushner, A. M.; Ziller, J.; Guan, Z., "Self-Healing Supramolecular Block Copolymers," Angew. Chem. Int. 51 (42), 10561–10565 (2012).

[9] Hillmyer, M. A.; Tolman, W. B., "Aliphatic Polyester Block Polymers: Renewable, Degradable, and Sustainable," Acc. Chem. Res. 47, 2390–2396 (2014).

[10] Scheutz, G. M.; Lessard, J. J.; Sims, M. B.; Sumerlin, B. S., "Adaptable Crosslinks in Polymeric Materials: Resolving the Intersection of Thermoplastics and Thermosets," J. Am. Chem. Soc. 141, 16181–16196 (2019).

[11] Bensabeh, N.; Jiménez-Alesanco, A.; Liblikas, I.; Ronda, J. C.; Cádiz, V.; Galià, M.; Vares, L.; Abián, O.; Lligadas, G., "Biosourced All-Acrylic ABA Block Copolymers with Lactic Acid-Based Soft Phase," Molecules 25, 5740 (2020).

[12] Shentu, Z.; Zhang, Z.; Zhao, J.; Chen, C.; Wu, Q.; Wang, L.; Yan, X., "Supramolecular Polymer-Assisted Manipulation of Triblock Copolymers: Understanding the Relationships between Microphase Structures and Mechanical Properties," J. Mater. Chem. A 9, 19619–19624 (2021).

[13] Bai, J.; Shi, Z.; Yin, J.; Tian, M., "Tailoring the Morphologies and Mechanical Properties of Styrene–Butadiene–Styrene Triblock Copolymers by the Incorporation of Thiol Functionalized Benzoxazine," Macromolecules 47, 2964–2973 (2014).

[14] Burns, A. B.; Register, R. A., "Thermoplastic Elastomers via Combined Crystallization and Vitrification from Homogeneous Melts," Macromolecules 49, 269–279 (2016).

[15] Kricheldorf, H. R., Quirk, R. P., Holden, G., Eds., "Thermoplastic Elastomers," Hanser Gardner Publications, (2004).

[16] Shipp, D. A.; Wang, J.-L.; Matyjaszewski, K., "Synthesis of Acrylate and Methacrylate Block Copolymers Using Atom Transfer Radical Polymerization," Macromolecules 31, 8005–8008 (1998).

[17] Jeusette, M.; Leclère, Ph.; Lazzaroni, R.; Simal, F.; Vaneecke, J.; Lardot, Th.; Roose, P., "New "All-Acrylate" Block Copolymers: Synthesis and Influence of the Architecture on the Morphology and the Mechanical Properties," Macromolecules 40, 1055–1065 (2007).

[18] Creton, C., "Pressure-Sensitive Adhesives: An Introductory Course," MRS Bull. 28, 434–439 (2003).

[19] Benedek, I., "Pressure-Sensitive Adhesives and Applications," 2nd ed., CRC Press, (2004).

[20] Leibler, L.; Rubinstein, M.; Colby, R. H., "Dynamics of Reversible Networks," Macromolecules 24, 4701–4707 (1991).

[21] Rubinstein, M.; Obukhov, S. P., "Power-Law-like Stress Relaxation of Block Copolymers: Disentanglement Regimes," Macromolecules 26, 1740–1750 (1993).
[22] Hahn, H.; Lee, J. H.; Balsara, N. P.; Garetz, B. A.; Watanabe, H., "Viscoelastic Properties of Aligned Block Copolymer Lamellae," Macromolecules 34, 8701–8709 (2001).
[23] Patel, A. J.; Narayanan, S.; Sandy, A.; Mochrie, S. G. J.; Garetz, B. A.; Watanabe, H.; Balsara, N. P., "Relationship between Structural and Stress Relaxation in a Block-Copolymer Melt," Phys. Rev. Lett. 96 (25), 257801 (2006).
[24] Takano, A.; Kamaya, I.; Takahashi, Y.; Matsushita, Y., "Effect of Loop/Bridge Conformation Ratio on Elastic Properties of the Sphere-Forming ABA Triblock Copolymers: Preparation of Samples and Determination of Loop/Bridge Ratio," Macromolecules 38, 9718–9723 (2005).
[25] Sbrescia, S.; Ju, J.; Engels, T.; Van Ruymbeke, E.; Seitz, M., "Morphological Origins of Temperature and Rate Dependent Mechanical Properties of Model Soft Thermoplastic Elastomers," J. Polym. Sci. 59, 477–493 (2021).
[26] Ahn, H.; Lee, Y.; Lee, H.; Han, Y. S.; Seong, B. S.; Ryu, D. Y., "Various Phase Behaviors of Weakly Interacting Binary Block Copolymer Blends," Macromolecules 46, 4454–4461 (2013).
[27] Wang, R.-Y.; Huang, J.; Guo, X.-S.; Cao, X.-H.; Zou, S.-F.; Tong, Z.-Z.; Xu, J.-T.; Du, B.-Y.; Fan, Z.-Q., "Closed-Loop Phase Behavior of Block Copolymers in the Presence of Competitive Hydrogen-Bonding and Coulombic Interaction," Macromolecules 51, 4727–4734 (2018).
[28] Yeh, C.-L.; Hou, T.; Chen, H.-L.; Yeh, L.-Y.; Chiu, F.-C.; Müller, A. J.; Hadjichristidis, N., "Lower Critical Ordering Transition of Poly(Ethylene Oxide)- Block -Poly(2-Vinylpyridine)," Macromolecules 44, 440–443 (2011).
[29] Mulhearn, W. D.; Register, R. A., "Lower Critical Ordering Transition of an All-Hydrocarbon Polynorbornene Diblock Copolymer," ACS Macro Lett. 6, 808–812 (2017).
[30] Pollard, M.; Russell, T. P.; Ruzette, A. V.; Mayes, A. M.; Gallot, Y., "The Effect of Hydrostatic Pressure on the Lower Critical Ordering Transition in Diblock Copolymers," Macromolecules 31, 6493-6498 (1998).
[31] Cho, J., "Microphase Separation upon Heating in Diblock Copolymer Melts," Macromolecules 34, 1001-1012 (2001).
[32] Mok, M. M.; Ellison, C. J.; Torkelson, J. M., "Effect of Gradient Sequencing on Copolymer Order–Disorder Transitions: Phase Behavior of Styrene/ n -Butyl Acrylate Block and Gradient Copolymers," Macromolecules 44, 6220–6226 (2011).
[33] Russell, T. P.; Karis, T. E.; Gallot, Y.; Mayes, A. M., "A Lower Critical Ordering Transition in a Diblock Copolymer Melt," Nature 368, 729–731 (1994).
[34] Lv, C.; Wang, R.; Gao, J.; Ding, N.; Dong, S.; Nie, J.; Xu, J.; Du, B., "PAA-b-PPO-b-PAA Triblock Copolymers with Enhanced Phase Separation and Inverse Order-to-Order Phase Transition upon Increasing Temperature," Polymer 185, 121982 (2019).
[35] Wang, R.-Y.; Zhang, Z.-K.; Guo, X.-S.; Cao, X.-H.; Zhang, T.-Y.; Tong, Z.-Z.; Xu, J.-T.; Du, B.-Y.; Fan, Z.-Q., "Mechanistic Study of the Influence of Salt Species on the Lower Disorder-to-Order Transition Behavior of Poly(Ethylene Oxide)- b -Poly(Ionic Liquid)/Salt Hybrids," Macromolecules 53, 4560–4567 (2020).
[36] Zhang, Z.-K.; Guo, X.-S.; Zhang, T.-Y.; Wang, R.-Y.; Du, B.-Y.; Xu, J.-T., "Hierarchical Structures with Double Lower Disorder-to-Order Transition and Closed-Loop Phase Behaviors in Charged Block Copolymers Bearing Long Alkyl Side Groups," Macromolecules 53, 8714–8724 (2020).
[37] Wang, R.-Y.; Guo, X.-S.; Fan, B.; Zou, S.-F.; Cao, X.-H.; Tong, Z.-Z.; Xu, J.-T.; Du, B.-Y.; Fan, Z.-Q., "Design and Regulation of Lower Disorder-to-Order Transition Behavior in the Strongly Interacting Block Copolymers," Macromolecules 51, 2302–2311 (2018).
[38] Di Pilla, S., "Slip and Fall Prevention: A Practical Handbook," Lewis Publishers: Boca Raton, 2003.
[39] Mok, M. M.; Pujari, S.; Burghardt, W. R.; Dettmer, C. M.; Nguyen, S. T.; Ellison, C. J.; Torkelson, J. M., "Microphase Separation and Shear Alignment of Gradient Copolymers: Melt Rheology and Small-Angle X-Ray Scattering Analysis," Macromolecules 41, 5818–5829 (2008).

[40] Nicolas, J.; Ruzette, A.-V.; Farcet, C.; Gérard, P.; Magnet, S.; Charleux, B., "Nanostructured Latex Particles Synthesized by Nitroxide-Mediated Controlled/Living Free-Radical Polymerization in Emulsion," Polymer 48, 7029–7040 (2007).

[41] Rana, D.; Bag, K.; Bhattacharyya, S. N.; Mandal, B. M., "Miscibility of Poly(Styrene-Co-Butyl Acrylate) with Poly(Ethyl Methacrylate): Existence of Both UCST and LCST," J. Polym. Sci. Part B Polym. Phys. 38, 369–375 (2000).

[42] Chalykh, A. E.; Nikulova, U. V.; Shcherbina, A. A., "Phase Equilibria in a Polystyrene-Poly(Butyl Acrylate) System," Polym. Sci. Ser. A 57, 445–451 (2015).

[43] Somani, R. H.; Shaw, M. T., "Miscibility of Acrylic Polymers in Polystyrene by Melt Titration," Macromolecules 14, 1549–1554 (1981).

[44] Mok, M. M.; Kim, J.; Wong, C. L. H.; Marrou, S. R.; Woo, D. J.; Dettmer, C. M.; Nguyen, S. T.; Ellison, C. J.; Shull, K. R.; Torkelson, J. M., "Glass Transition Breadths and Composition Profiles of Weakly, Moderately, and Strongly Segregating Gradient Copolymers: Experimental Results and Calculations from Self-Consistent Mean-Field Theory," Macromolecules 42, 7863–7876 (2009).

[45] Miwa, Y.; Usami, K.; Yamamoto, K.; Sakaguchi, M.; Sakai, M.; Shimada, S., "Direct Detection of Effective Glass Transitions in Miscible Polymer Blends by Temperature-Modulated Differential Scanning Calorimetry," Macromolecules 38, 2355–2361 (2005).

[46] Guo, Y.; Gao, X.; Luo, Y., "Mechanical Properties of Gradient Copolymers of Styrene and n -Butyl Acrylate," J. Polym. Sci. Part B Polym. Phys. 53, 860–868 (2015).

[47] Mark, J. E., Ed., "Physical Properties of Polymers Handbook," 2nd ed. Springer, (2006).

[48] Claudy, P.; Letoffe, J.; Camberlain, Y.; Pascault, J., "Glass transition of polystyrene versus molecular weight," Polym. Bull. 9, 208–215 (1983).

[49] Fredrickson, G. H.; Helfand, E., "Fluctuation Effects in the Theory of Microphase Separation in Block Copolymers," J. Chem. Phys. 87, 697–705 (1987).

[50] Mayes, A. M.; de la Cruz, M. O., "Concentration Fluctuation Effects on Disorder–Order Transitions in Block Copolymer Melts," J. Chem. Phys. 95, 4670–4677 (1991).

[51] Wang, X.; Dormidontova, E. E.; Lodge, T. P., "The Order−Disorder Transition and the Disordered Micelle Regime for Poly(Ethylenepropylene- b -Dimethylsiloxane) Spheres," Macromolecules 35, 9687–9697 (2002).

[52] Wang, J.; Wang, Z.-G.; Yang, Y., "Nature of Disordered Micelles in Sphere-Forming Block Copolymer Melts," Macromolecules 38, 1979–1988 (2005).

[53] Lee, S.; Gillard, T. M.; Bates, F. S., "Fluctuations, Order, and Disorder in Short Diblock Copolymers," AIChE J. 59, 3502–3513 (2013).

[54] Karis, T. E.; Russell, T. P.; Gallot, Y.; Mayes, A. M., "Rheology of the Lower Critical Ordering Transition," Macromolecules 28, 1129–1134 (1995).

[55] Pakula, T.; Koynov, K.; Boerner, H.; Huang, J.; Lee, H.; Pietrasik, J.; Sumerlin, B.; Matyjaszewski, K., "Effect of Chain Topology on the Self-Organization and the Mechanical Properties of Poly(n-Butyl Acrylate)-b-Polystyrene Block Copolymers," Polymer 52, 2576–2583 (2011).

[56] Flory, P. J., "Principles of Polymer Chemistry," Ithaca, (2006).

[57] Bates, F. S., "Block Copolymers near the Microphase Separation Transition. 2. Linear Dynamic Mechanical Properties," Macromolecules 17, 2607–2613 (1984).

[58] Li, Y.; Pyromali, C.; Zhuge, F.; Fustin, C.-A.; Gohy, J.-F.; Vlassopoulos, D.; Van Ruymbeke, E., "Dynamics of Entangled Metallosupramolecular Polymer Networks Combining Stickers with Different Lifetimes," J. Rheol. 66, (2022), in press.

[59] Zhuge, F.; Hawke, L. G. D.; Fustin, C.-A.; Gohy, J.-F.; van Ruymbeke, E., "Decoding the Linear Viscoelastic Properties of Model Telechelic Metallo-Supramolecular Polymers," J. Rheol. 61, 1245–1262 (2017).

[60] Han, C. D.; Kim, J., "Rheological Technique for Determining the Order–Disorder Transition of Block Copolymers," J. Polym. Sci. Part B Polym. Phys. 25, 1741–1764 (1987).

[61] Han, C. D.; Kim, J.; Kim, J. K., "Determination of the Order-Disorder Transition Temperature of Block Copolymers," Macromolecules 22, 383–394 (1989).

[62] Patrick, R. L.; Dekker, M., "Treatise on Adhesion and Adhesives," J. Appl. Polym. Sci. *2*, 219–260 (1969).

[63] Williams, M. L.; Landel, R. F.; Ferry, J. D., "The Temperature Dependence of Relaxation Mechanisms in Amorphous Polymers and Other Glass-Forming Liquids," J. Am. Chem. Soc. 77, 3701–3707 (1955).

[64] André, A.; Shahid, T.; Oosterlinck, F.; Clasen, C., "Investigating the Transition between Polymer Melts and Solutions in Nonlinear Elongational Flow," Macromolecules 54, 2797−2810 (2021).

πάντα ῥεῖ

Journal of Rheology ACCEPTED MANUSCRIPT

This is the author's peer reviewed, accepted manuscript. However, the online version of record will be different from this version once it has been copyedited and typeset.
PLEASE CITE THIS ARTICLE AS DOI: 10.1122/8.0000506

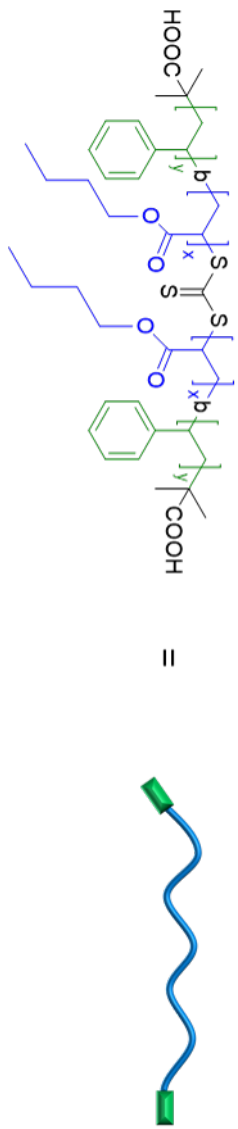

πάντα ῥεῖ

Journal of Rheology

ACCEPTED MANUSCRIPT

PLEASE CITE THIS ARTICLE AS DOI: 10.1122/8.0000506

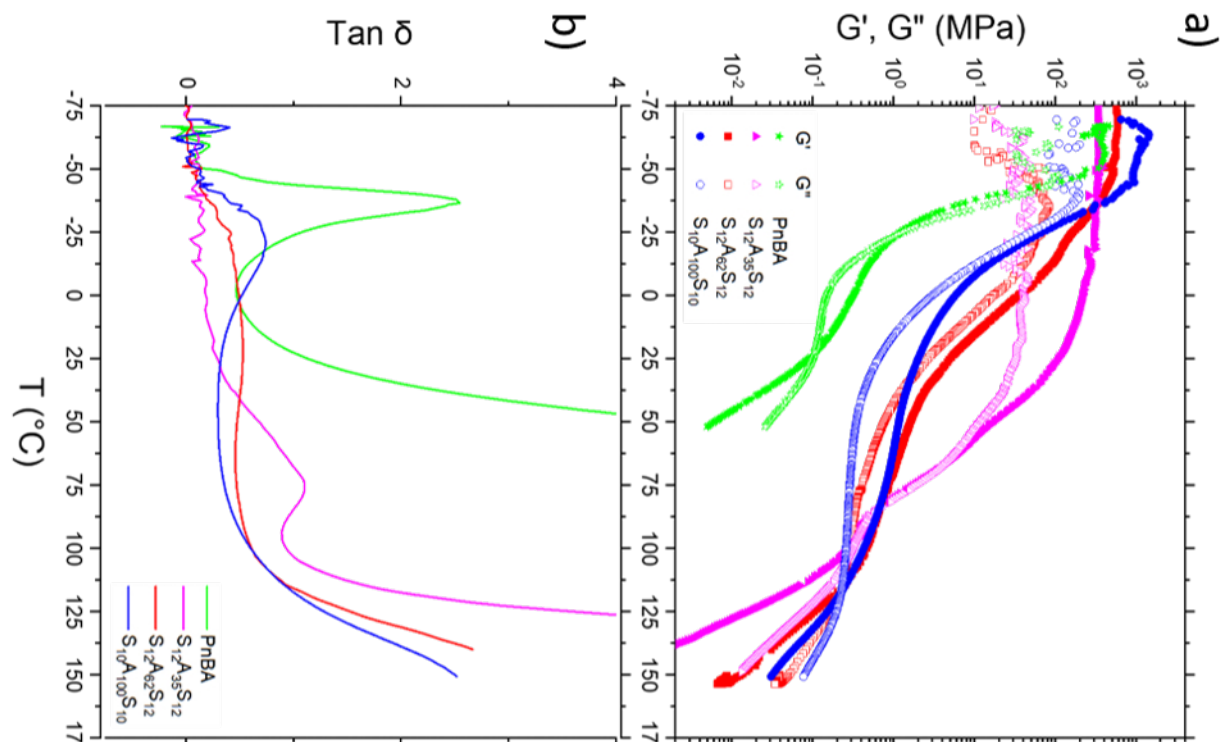

πάντα ῥεῖ

Journal of Rheology

ACCEPTED MANUSCRIPT

PLEASE CITE THIS ARTICLE AS DOI: 10.1122/8.0000506

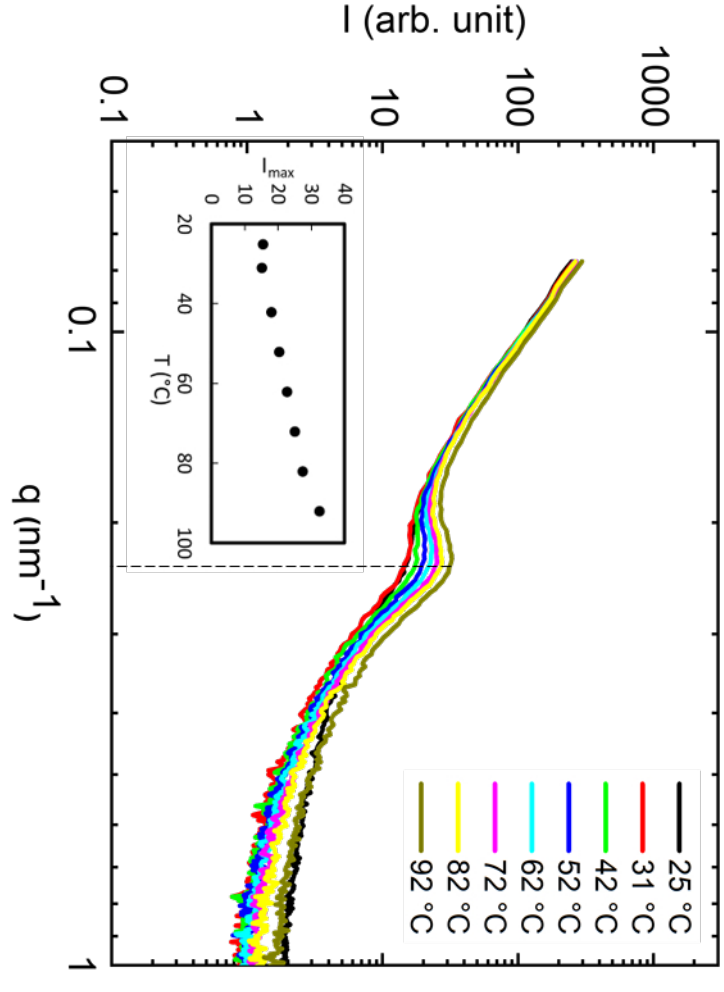

Journal of Rheology

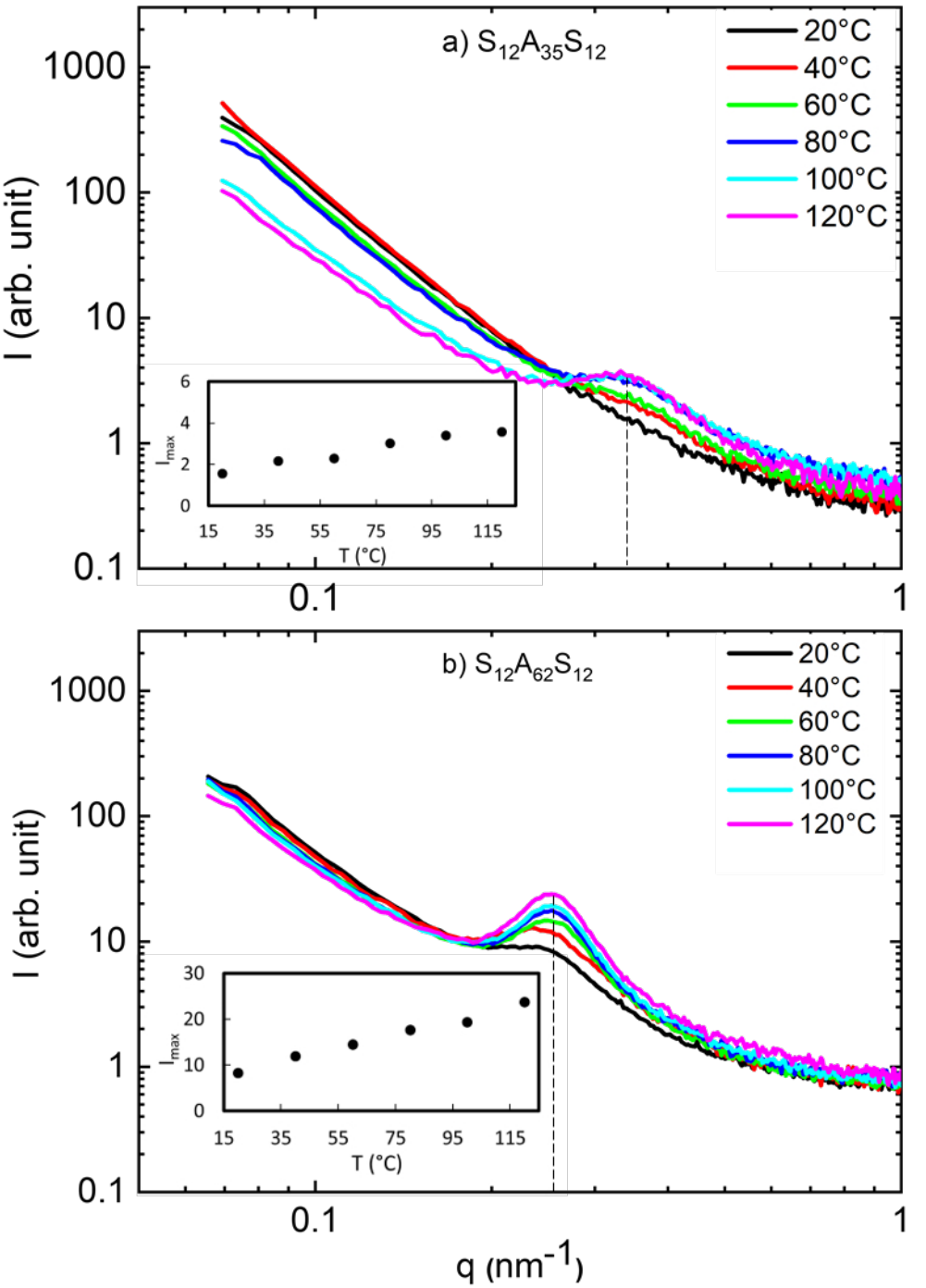

Journal of Rheology

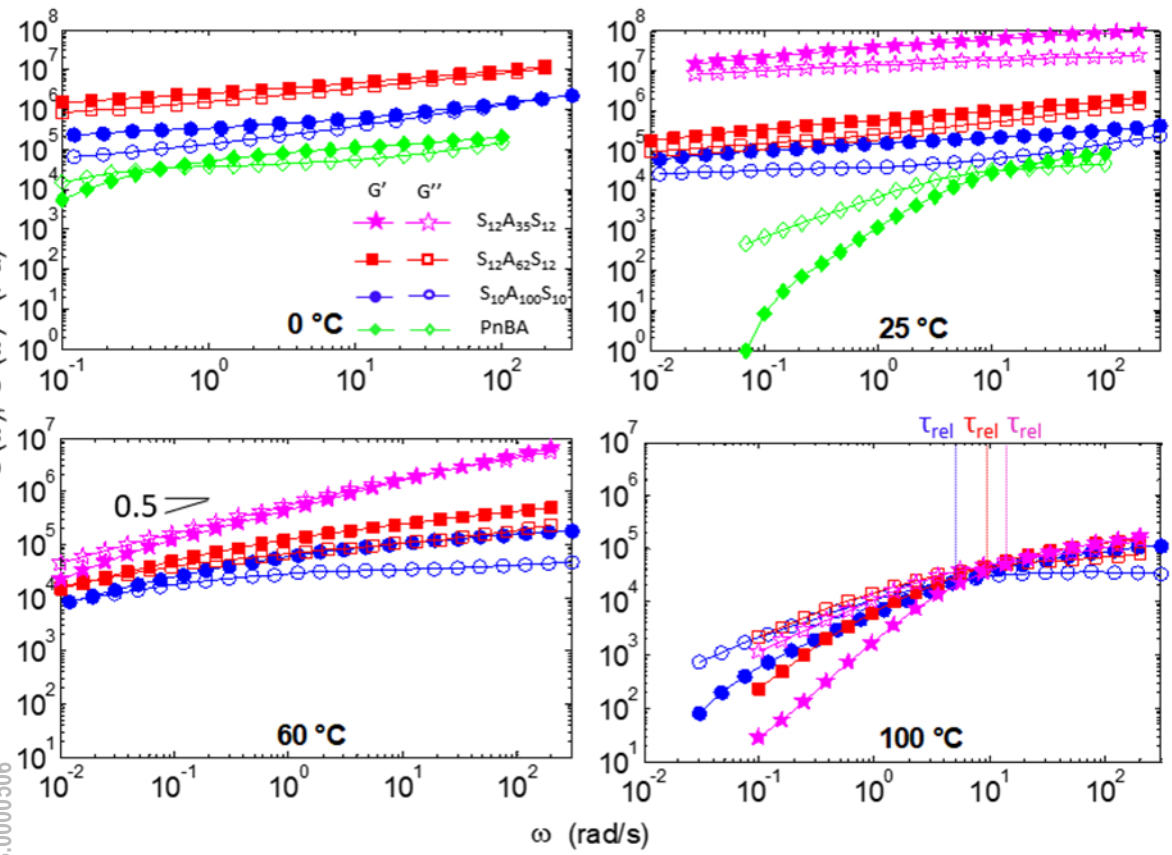

Journal of Rheology

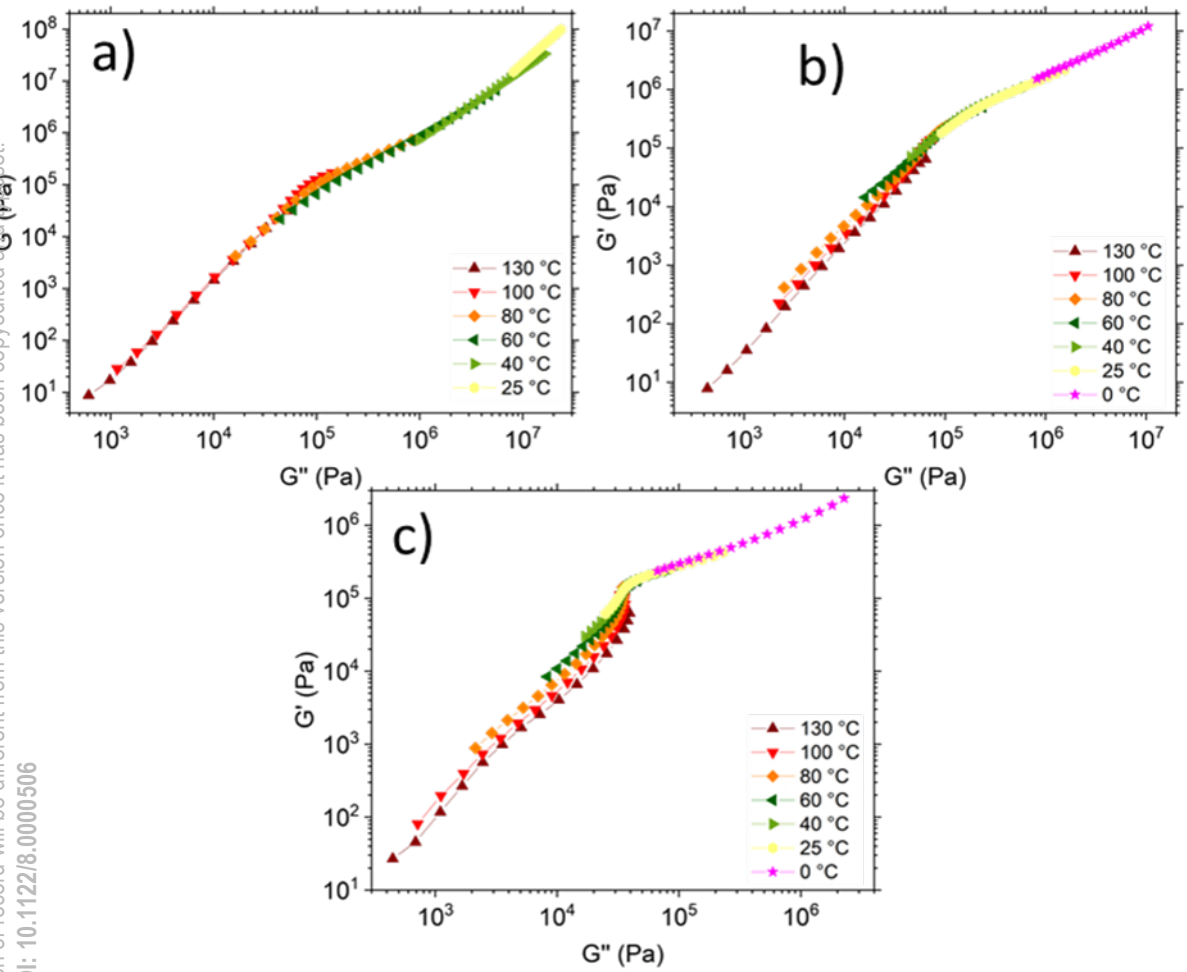

πάντα ῥεῖ

Journal of Rheology

ACCEPTED MANUSCRIPT

PLEASE CITE THIS ARTICLE AS DOI: 10.1122/8.0000506

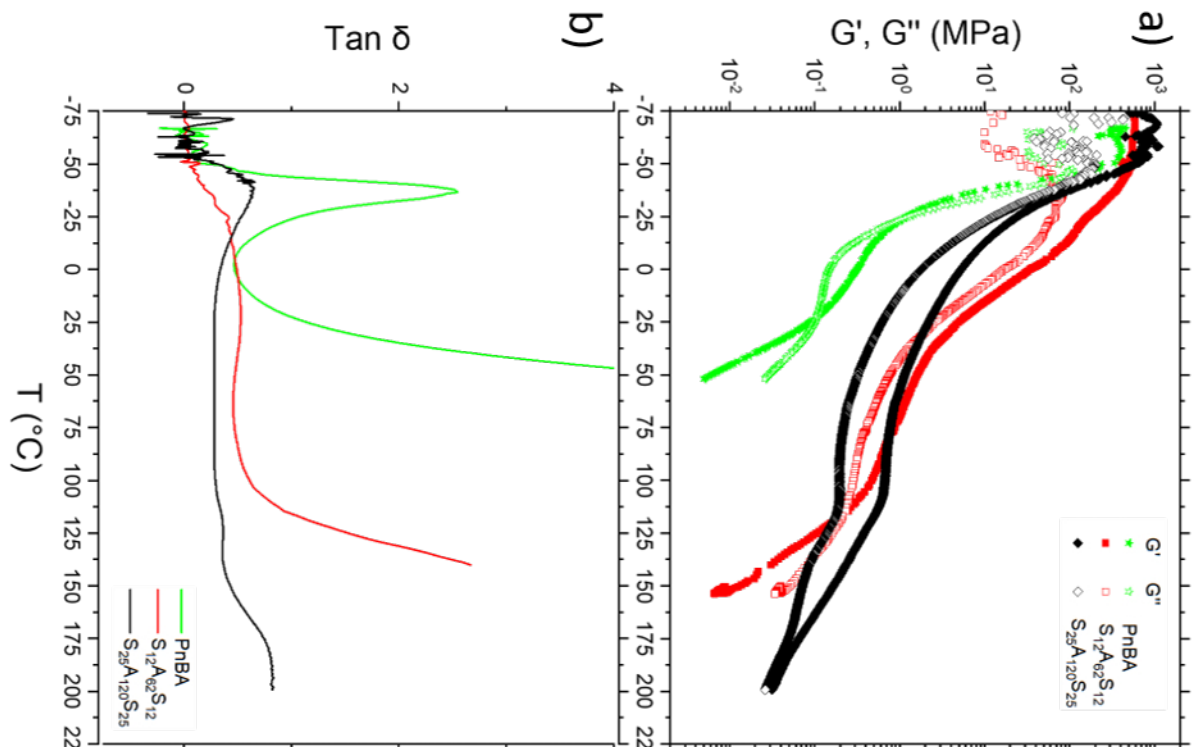

πάντα ῥεῖ

Journal of Rheology

ACCEPTED MANUSCRIPT

PLEASE CITE THIS ARTICLE AS DOI: 10.1122/8.0000506

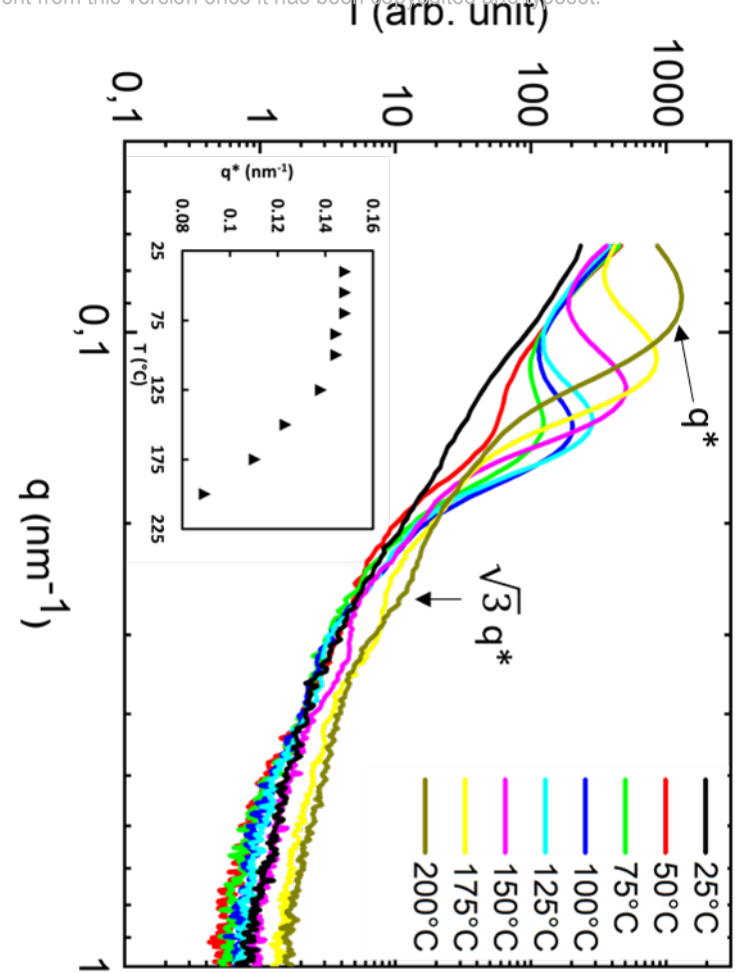

Journal of Rheology

πάντα ρεῖ

Journal of Rheology

ACCEPTED MANUSCRIPT

PLEASE CITE THIS ARTICLE AS DOI: 10.1122/8.0000506

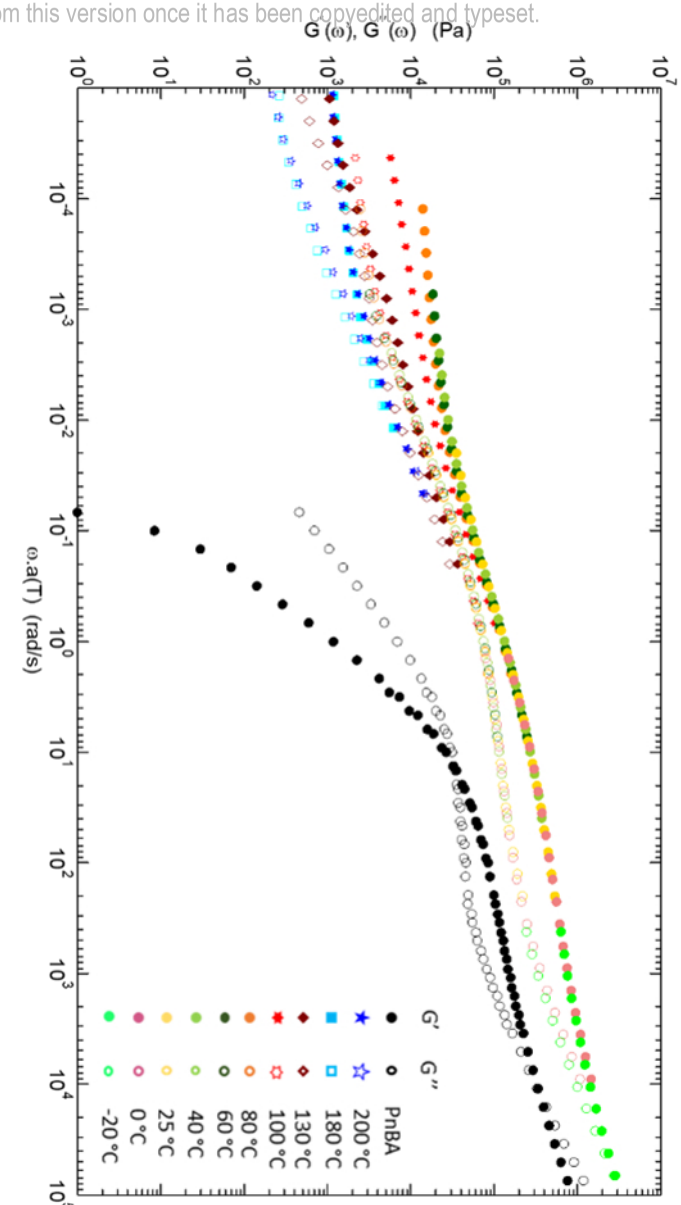

πάντα ῥεῖ

Journal of Rheology

ACCEPTED MANUSCRIPT

PLEASE CITE THIS ARTICLE AS DOI: 10.1122/8.0000506